Stabilisation of Parametric Roll Resonance by Combined Speed and Fin Stabiliser Control

Roberto Galeazzi*, Christian Holden†, Mogens Blanke*‡, Thor I. Fossen†‡

***Abstract*— Parametric roll resonance on a ship is a condition where large roll motion develops rapidly in moderate head or following seas. The phenomenon is caused by bifurcation in the nonlinear equations of motion when a restoring moment is subject to periodic variation. This paper analyzes the stability of the nonlinear system and suggests active control of both ship speed and fin stabilizers to stabilise the roll resonance condition. Lyapunov and backstepping designs are employed to achieve two nonlinear controllers, which are proved to stabilise the nonlinear system. The designed controllers are validated employing a high fidelity simulation model. The combined speed and fin stabiliser control is shown to efficiently drive the vessel out of the bifurcation condition and to quickly damp the residual roll motion.**

I. INTRODUCTION

Auto-parametric resonance is a de-stabilising effect, which can arise in mechanical systems consisting of two or more vibrating components [1]. This phenomenon can be described by

$$\ddot{x} + b(\dot{x})\dot{x} + a(t)x = 0 \tag{1}$$

where the parameter $a(t)$ is periodic, $a(t+T) = a(t)$. The conservative system (i.e $b = 0$) is recognised as the Hill-Mathieu's equation [2]. Equation (1) is subject to instabilities, which can occur when there is resonance between the imposed period T and the natural period T_0. The resonance condition is that T, or $2T$, is an integer multiple of T_0.

Parametric roll is an auto-parametric resonance phenomenon whose onset causes a sudden and quick rise in roll oscillations. The resulting large roll motion, which can reach 30-40 degrees of roll angle, may bring the vessel into conditions dangerous for the ship, the cargo, and the crew. The origin of this unstable motion is the time-varying geometry of the submerged hull, which produces periodic variations of the transverse stability properties of the ship. Container ships are known to be particularly prone to this phenomenon due to the hull shape – i.e. bow flare and stern overhang – which brings about dramatic variations in intercepted water-plane area when a wave crest or trough is close to amidships position. Incidents have been reported with significant damage to the cargo as well as to the ship [3], [4].

*Dept. of Electrical Engineering, Technical University of Denmark, 2800 Kgs. Lyngby, Denmark rg@elektro.dtu.dk, mb@elektro.dtu.dk

†Dept. of Engineering Cybernetics, Norwegian University of Science and Technology, 7491 Trondheim, Norway c.holden@ieee.org, fossen@ieee.org

‡Centre for Ships and Ocean Structures, Norwegian University of Science and Technology, 7491 Trondheim, Norway

Parametric roll is known to occur when a ship sails in moderate to heavy longitudinal or oblique seas; the wave passage along the hull and the wave excited vertical motions result in variations of the intercepted waterplane area, and in turn, in relevant changes in the roll restoring characteristics. The onset and buildup of parametric roll is due to the occurrence of concomitant conditions: the wave length is close to the ship length ($\lambda_w \approx L_s$), the ship approaches waves with encounter frequency of about twice the roll natural frequency ($\omega_e \approx 2\omega_\phi$), and the wave height is greater than a ship-dependent threshold ($h_w > \overline{h}_s$).

This work aims at designing a control strategy that is capable of stabilising the parametric roll motion to zero when the foregoing conditions are met. Different methods are available in order to stabilise the phenomenon using different actuators; e.g. active U-tanks are employed in [5] in order to drive the roll motion to zero.

The control strategy proposed in this paper relies on two factors: to vary the forward speed of the vessel in order to de-tune the frequency coupling condition ($\omega_e \approx 2\omega_\phi$), and to increase the roll damping by means of the fins. The two controllers are designed applying Lyapunov stability theory.

The analytical results are tested by simulations, using the benchmark model of [6].

II. MODEL

A nonlinear coupled surge-roll model is set up where the interaction between the two modes is presented in terms of a time-varying wave encounter frequency.

The standard definition of wave encounter frequency is based on the assumption of constant ship forward speed U

$$\omega_e \triangleq \omega - kU\cos\chi, \tag{2}$$

where ω is the wave frequency, k is the wave number, and χ is the encounter angle. The definition (2) was shown to be valid also when a time-varying forward speed is taken into account [7].

Some important assumptions for the development of the model are:

- the vessel is sailing in head seas ($\chi = 180°$);
- sway motion is neglected, therefore the time-varying forward speed U can be approximated as

  $$U(t) = \sqrt{u(t)^2 + v(t)^2} \approx u(t), \tag{3}$$

  where u and v are the surge and sway velocities, respectively;

- the 1st-order wave excitation forces are considered only in terms of the Froude-Krylov forces, disregarding the diffraction forces.

A. Surge Mode

For a vessel sailing in head seas, the forces acting along the longitudinal direction are: the inertial forces due to mass and added mass, the drag forces due to wave resistance, the thrust supplied by the propeller, and the external forces due to the incident waves under the assumption that the hull is restrained from moving. The non-linear surge dynamics is, to a first order approximation, where wave pressure generated forces are considered and thrust deduction from propeller flow around the stern are included but wave reflection and drag terms from hull motions and the rudder are disregarded,

$$(m - X_{\dot{u}})\dot{u} = R(u) + (1 - t_d)T_p + F_x^{FK}, \qquad (4)$$

where m is the ship's mass, $-X_{\dot{u}} > 0$ the added mass term, $R(u)$ the ship's non-linear hydrodynamic resistance, T_p the propeller thrust, $t_d \in [0\ ,\ 1]$ the thrust deduction factor, and F_x^{FK} the longitudinal Froude-Krylov force created by wave pressure integrated over the hull. The latter is a nonlinear term since wave pressure increases with wave elevation and the area over which to integrate forces also increase by wave elevation.

The ship resistance function $R(u)$ provides damping in surge and consists of linear laminar skin friction $X_u u$, and of nonlinear quadratic drag $X_{|u|u}\,|u|\,u$ [8]

$$R(u) = X_u u + X_{|u|u}\,|u|\,u < 0. \qquad (5)$$

Higher order terms in $R(u)$ occur due to wave making in the high end of range of ship speed, but this is not essential in this context.

According to linear airy theory [9], the wave induced force in surge is taken as the longitudinal Froude-Krylov force, considering the incident wave pressure in a regular wave. Therefore, the 1st-order wave excitation force in surge is given according to [10] by

$$\begin{aligned} F_x^{FK} &= \int_V \frac{\partial p(X,Z,t)}{\partial x}\,\mathrm{d}V \qquad (6)\\ &= \gamma_1 \omega_e(t)\Big[\sin\Big(\omega t + kL_s + k\int_0^t U(\tau)\,\mathrm{d}\tau\Big)\\ &\quad - \sin\Big(\omega t + k\int_0^t U(\tau)\,\mathrm{d}\tau\Big)\Big]. \end{aligned}$$

where $\gamma_1 = B\frac{\rho g \bar{\zeta}}{k\omega}(1 - e^{-kT})$, ρ is the water density, $\bar{\zeta}$ the wave amplitude, L_s the ship length, B the ship breadth, and T the ship draught.

B. Roll Mode

Models of different complexity have been presented in literature in order to describe the roll mode in parametric resonance condition. The simplest way to model parametric roll is to consider the uncoupled non-linear equation of roll

$$(I_{xx} - K_{\ddot{\phi}})\ddot{\phi} + \bar{K}_{\dot{\phi}}(\dot{\phi})\dot{\phi} + mg\mathrm{GM}(t)\phi + K_{\phi^3}\phi^3 = 0 \quad (7)$$

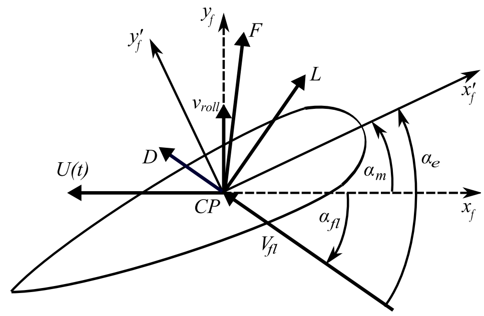

Fig. 1. Fin motion induced by roll motion

and to recast it as the nonlinear damped Mathieu's Equation, as shown in [11]. In (7) I_{xx} is the ship's inertia, $-K_{\ddot{\phi}} > 0$ the added inertia, $\bar{K}_{\dot{\phi}}(\dot{\phi})\dot{\phi}$ the hydrodynamic damping that can be expressed as

$$\bar{K}_{\dot{\phi}}(\dot{\phi})\dot{\phi} = -(K_{\dot{\phi}}\dot{\phi} + K_{|\dot{\phi}|\dot{\phi}}|\dot{\phi}|\dot{\phi}) > 0, \qquad (8)$$

$K_{\phi^3} > 0$ the nonlinear spring term. The time-varying restoring moment is $mg\mathrm{GM}(t)$, with the metacentric height defined as

$$\mathrm{GM}(t) \triangleq \overline{\mathrm{GM}} + \mathrm{GM}_a \cos(\omega_e t) \qquad (9)$$

where $\overline{\mathrm{GM}}$ is the still water metacentric height, and GM_a is the amplitude of the variation of the metacentric height in waves.

A 3rd-order nonlinear coupled model has been developed in [6], where roll is fully coupled with the motions in the vertical plane. Let $\xi = [z,\ \phi,\ \theta]^{\mathrm{T}}$ be the generalised coordinate vector, where z is the heave displacement, ϕ is the roll angle, and θ is the pitch angle. Then the nonlinear equation of motion in matrix form are given by

$$(\mathbf{M} + \mathbf{A})\ddot{\xi} + \mathbf{D}(\dot{\phi})\dot{\xi} + \mathbf{c}_{\mathrm{res}}(\xi, t) = \mathbf{c}_{\mathrm{ext}}(t). \qquad (10)$$

Further details – included numerical values of model parameters for a 281 m, 76500 tonnes container ship – can be found in [6]. This model is used to verify the designed control law.

C. Fins Model

Fins give rise to a moment acting on roll [12] given as

$$\tau_\phi = 2Nr_f, \qquad (11)$$

where N is the normal component of the total hydrodynamic force F resulting from lift force L and drag force D acting on the centre of pressure (CP) of the fin (see Fig. 1), and r_f is the fin roll arm. The magnitude of τ_ϕ is related to the effective angle of attack α_e of the fin. The normal component of F is given by

$$N = L\cos\alpha_e + D\sin\alpha_e, \qquad (12)$$

where the lift force L is

$$L = \frac{1}{2}\rho V_f^2 S C_L(\alpha_e) \qquad (13)$$

with V_f being the flow velocity, S the fin surface, and C_L the lift coefficient, and D is the drag force.

The fins are commanded by hydraulic machinery that can be modeled as a first order system with saturation effects (see [12], [13]). Therefore, it is assumed that a first order model can be employed in order to dynamically describe the generation of the fin-induced roll moment τ_ϕ

$$\dot{\tau}_\phi + \frac{1}{t_r}\tau_\phi = \frac{1}{t_r}\tau_{\max}\mathrm{sat}\left(\frac{\tau_c}{\tau_{\max}}\right), \tag{14}$$

where $\tau_{\max}$ is the maximum moment that can be produced by the fins taking into account saturation effects on the mechanical angle and on the lift coefficient, and τ_c is the moment commanded by the controller. The time constant t_r is assumed to be the same as that of the hydraulic machinery since the moment cannot be changed at a rate faster than the fins can move.

D. Resulting Models

Two models are then employed for the design and the analysis of the control system. A reduced model, where roll is only coupled with surge, is first used to design a controller capable of varying the ship forward speed and drive the roll motion to zero. Then, a 4-DOF surge-heave-roll-pitch high fidelity model is employed to evaluate the performance of the controllers.

1) Plant Model: The plant is described by a 4-DOF model based upon the 3rd-order model developed in [6], where surge, heave, roll, and pitch are coupled together. Let $\bar{\xi} = [x, \xi^T]^{\mathrm{T}}$ be the generalised coordinate vector, then the equation of motions in matrix form are

$$\begin{aligned}(\bar{\mathbf{M}} + \bar{\mathbf{A}})\ddot{\bar{\xi}} + \bar{\mathbf{D}}(u,\dot{\phi})\dot{\bar{\xi}} + \bar{\mathbf{c}}_{\mathrm{res}} &= \bar{\mathbf{c}}_{\mathrm{ext}} + \mathbf{f} \\ \dot{\tau}_\phi + \frac{1}{t_r}\tau_\phi &= \frac{1}{t_r}\tau_{\max}\mathrm{sat}\left(\frac{\tau_c}{\tau_{\max}}\right)\end{aligned} \tag{15}$$

where

$$\begin{aligned}\bar{\mathbf{M}} &= \mathrm{diag}(m, m, I_{xx}, I_{yy}) \\ \bar{\mathbf{A}} &= -\begin{bmatrix} X_{\dot{u}} & \mathbf{0}_{1\times3} \\ \mathbf{0}_{3\times1} & \mathbf{A}\end{bmatrix} > 0 \\ \bar{\mathbf{D}}(u,\dot{\phi}) &= -\begin{bmatrix} R(u) & \mathbf{0}_{1\times3} \\ \mathbf{0}_{3\times1} & \mathbf{D}(\dot{\phi})\end{bmatrix} > 0 \\ \bar{\mathbf{c}}_{\mathrm{res}} &= [0,\, \mathbf{c}_{\mathrm{res}}(\xi,\dot{\xi},t)]^{\mathrm{T}} \\ \bar{\mathbf{c}}_{\mathrm{ext}} &= [F_x^{FK}(\dot{\xi},t),\, \mathbf{c}_{\mathrm{ext}}(t)]^{\mathrm{T}} \\ \mathbf{f} &= [f_1(u_d,\dot{u}_d,u),\, 0,\, f_2(\phi,\dot{\phi},\ddot{\phi}),\, 0]^{\mathrm{T}}.\end{aligned}$$

2) Nominal Model: The nominal model is based on a surge-roll coupled system where the coupling between the two modes is given by the time-varying encounter frequency.

Let $\eta \triangleq [x,\, \phi]^{\mathrm{T}}$ and $\nu \triangleq \dot{\eta} = [u,\, p]^{\mathrm{T}}$ be the generalised position and velocity vectors, respectively. Then, with $\tau = [\tau_u,\, \tau_\phi]^{\mathrm{T}}$ being the control input vector, the control model reads

$$\begin{aligned}\dot{\eta} &= \nu \\ \mathcal{M}\dot{\nu} + \mathcal{D}(\nu)\nu + \mathcal{K}(\eta,\nu,t)\eta + e(\nu,t) &= \tau \\ \dot{\tau}_\phi + \frac{1}{t_r}\tau_\phi &= \frac{1}{t_r}\tau_{\max}\mathrm{sat}\left(\frac{\tau_c}{\tau_{\max}}\right)\end{aligned} \tag{16}$$

where

$$\begin{aligned}\mathcal{M} &= \begin{bmatrix} m - X_{\dot{u}} & 0 \\ 0 & I_{xx} - K_{\ddot{\phi}}\end{bmatrix} \\ \mathcal{D}(\nu) &= -\begin{bmatrix} X_u + X_{|u|u}|\nu_1| & 0 \\ 0 & K_{\dot{\phi}} + K_{|\dot{\phi}|\dot{\phi}}|\nu_2|\end{bmatrix} \\ \mathcal{K}(\eta,\nu,t) &= \begin{bmatrix} 0 & 0 \\ 0 & \mathcal{K}_{22,\nu_1} + \mathcal{K}_{22,\eta_2}\end{bmatrix} \\ e(\nu,t) &= \begin{bmatrix} -F_x^{FK}(\nu_1,t) \\ 0\end{bmatrix}\end{aligned}$$

where $\mathcal{K}_{22,\nu_1} = mg\mathrm{GM}(\nu_1,t)$, and $\mathcal{K}_{22,\eta_2} = K_{\phi^3}\eta_2^2$.

III. ANALYSIS AND DESIGN

The design of the speed controller is done by applying classical Lyapunov stability theory, whereas the fin stabiliser is designed by applying backstepping [14].

A. Speed Controller

Given the surge subsystem

$$\dot{\nu}_1 = -\mathcal{D}'_{11}(\nu_1)\nu_1 - e'_1(\nu_1,t) + \tau'_u \tag{17}$$

where $\mathcal{D}'_{11}(\nu_1) = \frac{\mathcal{D}_{11}(\nu_1)}{\mathcal{M}_{11}}$, $e'_1(\nu_1,t) = \frac{e_1(\nu_1,t)}{\mathcal{M}_{11}}$, and $\tau'_u = \frac{\tau_u}{\mathcal{M}_{11}}$. The control goal is to design the controller τ'_u capable of varying the forward speed $U(t)$ so that the parametric resonance condition $\omega_e \approx 2\omega_\phi$ is avoided. This will push the system out of the instability region where parametric roll can occur.

Defining the error dynamics as

$$z_1 = \nu_1 - \nu_d, \tag{18}$$

where z_1 is the tracking error and $\nu_d \in C^1$ is a bounded reference trajectory, then (17) can be rewritten as

$$\begin{aligned}\dot{z}_1 &= \dot{\nu}_1 - \dot{\nu}_d \\ &= -\mathcal{D}'_{11}(\nu_1)(z_1 + \nu_d) - e'_1(\nu_1,t) + \tau'_u - \dot{\nu}_d.\end{aligned} \tag{19}$$

The control Lyapunov function for the system (19) is

$$V_1 = \frac{1}{2}\mathcal{M}_{11}z_1^2, \tag{20}$$

which is positive definite and radially unbounded; hence there exist class $\mathcal{K}_\infty$ functions α_1 and α_2 such that V_1 satisfies the following relationship globally

$$\alpha_1(|z_1|) \leq V_1 \leq \alpha_2(|z_1|). \tag{21}$$

The derivative of V_1 along the trajectories of the system is given by

$$\begin{aligned}\dot{V}_1 = z_1(&-\mathcal{D}_{11}(\nu_1)(z_1 + \nu_d) - e_1(\nu_1,t) + \tau_u \\ &- \mathcal{M}_{11}\dot{\nu}_d).\end{aligned} \tag{22}$$

Choosing the control input τ_u to be

$$\tau_u = \mathcal{D}_{11}(\nu_1)\nu_d + \mathcal{M}_{11}\dot{\nu}_d - \kappa_1 z_1,\ \forall\, \kappa_1 > 0 \tag{23}$$

gives

$$\dot{V}_1 = -(\kappa_1 + \mathcal{D}_{11}(\nu_1))z_1^2 - e_1(\nu_1,t)z_1. \tag{24}$$

The disturbance $e_1(\nu_1,t)$ satisfies the following relationship (see Appendix A)

$$e_1(\nu_1,t) \le 2\gamma_1\omega + 2\gamma_1 k z_1 + 2\gamma_1 k \nu_{d,\max}. \tag{25}$$

Therefore, the following inequality holds

$$\begin{aligned}
\dot V_1 &\le -(\mathcal{D}_{11}(\nu_1) + \kappa_1 - 2\gamma_1 k) z_1^2 \\
&\quad + 2\gamma_1(\omega + k\nu_{d,\max})|z_1| \\
&\le -(1-\theta_1)(\mathcal{D}_{11}(\nu_1) + \kappa_1 - 2\gamma_1 k) z_1^2 \\
&\quad - \theta_1(\mathcal{D}_{11}(\nu_1) + \kappa_1 - 2\gamma_1 k) z_1^2 + 2\gamma_1(\omega + k\nu_{d,\max})|z_1| \\
&\le -(1-\theta_1)(\mathcal{D}_{11}(\nu_1) + \kappa_1 - 2\gamma_1 k) z_1^2 \\
&\le -(1-\theta_1)(-X_u + \kappa_1 - 2\gamma_1 k) z_1^2
\end{aligned} \tag{26}$$

$\forall\ |z_1| > \mu$ and $\forall \kappa_1 > X_u + 2\gamma_1 k$, where $\mu \triangleq \frac{2\gamma 1(\omega + k\nu_{d,\max})}{\theta_1(-X_u+\kappa_1-2\gamma_1 k)}$, and $\theta_1 \in (0,1)$. Hence, the solutions are globally uniformly ultimately bounded [14, Theorem 4.18]. In order to find the ultimate bound the functions $\alpha_1(|z_1|)$ and $\alpha_2(|z_1|)$ must be determined. Using

$$\alpha_1(|z_1|) = \alpha_2(|z_1|) = \frac{1}{2}\mathcal{M}_{11} z_1^2, \tag{27}$$

then the ultimate bound is given by

$$b = \alpha_1^{-1}(\alpha_2(\mu)) = \mu. \tag{28}$$

B. Fin Stabiliser

Given the roll subsystem

$$\dot\eta_2 = \nu_2 \tag{29a}$$

$$\dot\nu_2 = -\mathcal{D}'_{22}(\nu_2)\nu_2 - \mathcal{K}'_{22}\eta_2 + \tau'_\phi \tag{29b}$$

$$\dot\tau_\phi = -\frac{1}{t_r}\tau_\phi + \frac{1}{t_r}\tau_{\max}\mathrm{sat}\left(\frac{\tau_c}{\tau_{\max}}\right) \tag{29c}$$

where $\mathcal{D}'_{22}(\nu_2) = \frac{\mathcal{D}_{22}(\nu_2)}{\mathcal{M}_{22}}$, $\mathcal{K}'_{22} = \frac{\mathcal{K}_{22}}{\mathcal{M}_{22}}$, and $\tau'_\phi = \frac{\tau_\phi}{\mathcal{M}_{22}}$, the control goal is to stabilise the roll angle η_2 to zero.

1) First Step: For the system (29a) the state variable ν_2 is considered as virtual control input. The control Lyapunov function is

$$V_1(\eta_2) = \frac{1}{2}c_1\eta_2^2 \tag{30}$$

$$\dot V_1 = c_1\eta_2\nu_2, \tag{31}$$

where c_1 is a positive real constant. Therefore, choosing

$$\nu_2 = \psi_1(\eta_2) = -\kappa_2\eta_2, \tag{32}$$

with $\kappa_2 > 0$ gives

$$\dot V_1 = -\kappa_2 c_1 \eta_2^2 < 0 \tag{33}$$

and the origin of (29a) is globally exponentially stable [14].

2) Second Step: The subsystem (29a), (29b) is considered. The new state variable $z_2 = \nu_2 - \psi_1(\eta_2) = \nu_2 + \kappa_2\eta_2$ is introduced. Its time derivative is $\dot z_2 = \dot\nu_2 + \kappa_2\nu_2$. The control Lyapunov function is chosen as

$$V_2(\eta_2, z_2) = V_1(\eta_2) + \frac{1}{2}\mathcal{M}_{22} z_2^2 \tag{34}$$

$$\begin{aligned}
\dot V_2 &= -\kappa_2 c_1\eta_2^2 + z_2(-\mathcal{D}_{22}(\nu_2)(z_2 - \kappa_2\eta_2) \\
&\quad - \mathcal{K}_{22}\eta_2 + \tau_\phi + \mathcal{M}_{22}\kappa_2(z_2 - \kappa_2\eta_2)).
\end{aligned} \tag{35}$$

Hence, choosing the fin-induced roll moment to be

$$\begin{aligned}
\tau_\phi = \psi_2(\eta_2, z_2) &= -\kappa_3 z_2 - \mathcal{D}_{22}(\nu_2)\kappa_2\eta_2 + \mathcal{K}_{22,\eta_2}\eta_2 \\
&\quad - \mathcal{M}_{22}\kappa_2(z_2 - \kappa_2\eta_2),\ \forall\ \kappa_3 > 0
\end{aligned} \tag{36}$$

then $\dot V_2$ reads

$$\begin{aligned}
\dot V_2 &= -\kappa_2 c_1\eta_2^2 - (\mathcal{D}_{22}(\nu_2) + \kappa_3) z_2^2 \\
&\quad - \mathcal{K}_{22,\nu_1}\eta_2 z_2.
\end{aligned} \tag{37}$$

Defining $\gamma_2 \triangleq mg\overline{\mathrm{GM}} > 0$ and $\gamma_3 \triangleq mg\mathrm{GM}_a > 0$, then the roll restoring moment $K_{22}(\nu_1, t)$ satisfies the following inequality

$$\mathcal{K}_{22,\nu_1} \le \gamma_2 + \gamma_3|\cos((\omega + k\nu_1)t)| \le \gamma_4, \tag{38}$$

where $\gamma_4 = \gamma_2 + \gamma_3$. Therefore $\dot V_2$ reads

$$\begin{aligned}
\dot V_2 &\le -\kappa_2 c_1\eta_2^2 - (\mathcal{D}_{22}(\nu_2) + \kappa_3) z_2^2 + \gamma_4|\eta_2||z_2| \\
&= -(1-\theta_2)\kappa_2 c_1\eta_2^2 - \theta_2\kappa_2 c_1\eta_2^2 - (\mathcal{D}_{22}(\nu_2) + \kappa_3) z_2^2 \\
&\quad + \gamma_4|\eta_2||z_2| \\
&= -(1-\theta_2)\kappa_2 c_1\eta_2^2 - \left(\sqrt{\theta_2\kappa_2 c_1}|\eta_2| - \frac{\gamma_4}{2\sqrt{\theta_2\kappa_2 c_1}}|z_2|\right)^2 \\
&\quad + \frac{\gamma_4^2}{4\theta_2\kappa_2 c_1} z_2^2 - (\mathcal{D}_{22}(\nu_2) + \kappa_3) z_2^2 \\
&\le -(1-\theta_2)\kappa_2 c_1\eta_2^2 - \left(\mathcal{D}_{22}(\nu_2) + \kappa_3 - \frac{\gamma_4^2}{4\theta_2\kappa_2 c_1}\right) z_2^2 \\
&\le -(1-\theta_2)\kappa_2 c_1\eta_2^2 - \left(-K_{\dot\phi} + \kappa_3 - \frac{\gamma_4^2}{4\theta_2\kappa_2 c_1}\right) z_2^2.
\end{aligned} \tag{39}$$

that is negative definite for $\forall\ \kappa_3 > \frac{\gamma_4^2}{4\theta_2\kappa_2 c_1} + K_{\dot\phi}$ with $\theta_2 \in (0,1)$.

3) Third Step: The subsystem (29a), (29b), (29c) is finally taken into account. To back-step the change of variable

$$\begin{aligned}
z_3 &= \tau_\phi - \psi_2(\eta_2, z_2) \\
&= \tau_\phi + \kappa_3 z_2 + \mathcal{D}_{22}(\nu_2)\kappa_2\eta_2 + \mathcal{M}_{22}\kappa_2(z_2 - \kappa_2\eta_2) \\
&\quad + \mathcal{K}_{22,\eta_2}\eta_2
\end{aligned} \tag{40}$$

$$\dot z_3 = \dot\tau_\phi - \frac{\partial\psi_2}{\partial\eta_2}\dot\eta_2 - \frac{\partial\psi_2}{\partial z_2}\dot z_2 \tag{41}$$

is applied, where

$$\frac{\partial\psi_2}{\partial\eta_2} = -\kappa_2(\mathcal{D}_{22}(\nu_2) - \mathcal{M}_{22}\kappa_2) + 3\mathcal{K}_{22,\eta_2} \tag{42}$$

$$\frac{\partial\psi_2}{\partial z_2} = -(\kappa_3 + \mathcal{M}_{22}\kappa_2). \tag{43}$$

After introducing z_3, the system reads

$$\begin{aligned}
\dot\eta_2 &= \nu_2 \\
\dot\nu_2 &= -\mathcal{D}'_{22}(\nu_2)\nu_2 - \mathcal{K}'_{22}\eta_2 + \tau'_\phi \\
\dot z_3 &= -\frac{1}{t_r}\tau_\phi + \frac{1}{t_r}\tau_{\max}\mathrm{sat}\left(\frac{\tau_c}{\tau_{\max}}\right) - \frac{\partial\psi_2}{\partial\eta_2}\dot\eta_2 - \frac{\partial\psi_2}{\partial z_2}\dot z_2.
\end{aligned}$$

Substituting (40) into $\dot z_3$ gives

$$\begin{aligned}
\dot z_3 &= \frac{1}{t_r}\tau_{\max}\mathrm{sat}\left(\frac{\tau_c}{\tau_{\max}}\right) - \frac{\partial\psi_2}{\partial\eta_2}\dot\eta_2 - \frac{\partial\psi_2}{\partial z_2}\dot z_2 \\
&\quad - \frac{1}{t_r}(z_3 - \kappa_3 z_2 - \mathcal{D}_{22}(\nu_2)\kappa_2\eta_2 + \mathcal{K}_{22,\eta_2}\eta_2 \\
&\quad - \mathcal{M}_{22}\kappa_2(z_2 - \kappa_2\eta_2)).
\end{aligned} \tag{44}$$

TABLE I

SIMULATION PARAMETERS

Fin	Controllers
$S = 16.6 \text{ m}^2$	$\kappa_1 = 10^8 \text{ kgms}^{-1}$
$\dot{\alpha}_{\max} = 15.8 \deg \text{ s}^{-1}$	$c_1 = 6.5 \cdot 10^7 \text{ kgm}^2\text{s}^{-2}$
$\alpha_{\text{pb}} = 5 \deg$	$\kappa_2 = 1 \text{ s}^{-1}$
$t_r = \alpha_{\text{pb}}/\dot{\alpha}_{\max} \approx 0.32 \text{ s}$	$\kappa_3 \approx 3.24 \cdot 10^{10} \text{ kgm}^2\text{s}^{-2}$
	$\kappa_4 = 1$

Using the composite Lyapunov function

$$V_3(\eta_2, z_2, z_3) = V_2(\eta_2, z_2) + \frac{1}{2}z_3^2 \tag{45}$$

$$\begin{aligned}\dot{V}_3 &= \dot{V}_2 + z_3\dot{z}_3 \qquad (46)\\ &\leq -(1-\theta_2)\kappa_2 c_1 \eta_2^2 - z_3\left(\frac{\partial\psi_2}{\partial z_2}\dot{z}_2 + \frac{\partial\psi_2}{\partial\eta_2}\dot{\eta}_2\right)\\ &\quad + \frac{1}{t_r}z_3(\tau_c - z_3 + \kappa_3 z_2 + \mathcal{D}_{22}(\nu_2)\kappa_2\eta_2\\ &\quad + \mathcal{M}_{22}\kappa_2(z_2 - \kappa_2\eta_2))\\ &\quad - \left(-K_{\dot{\phi}} + \kappa_3 - \frac{\gamma_4^2}{4\theta_2\kappa_2 c_1}\right)z_2^2\end{aligned}$$

assuming $|\tau_c| \leq \tau_{\max}$. Selecting the control input τ_c as

$$\begin{aligned}\tau_c = \psi_3(\eta_2, z_2, z_3) &= -\kappa_3 z_2 - \kappa_2\mathcal{D}_{22}(\nu_2)\eta_2 \qquad (47)\\ &\quad - \mathcal{M}_{22}\kappa_2(z_2 - \kappa_2\eta_2)\\ &\quad + t_r\left(\frac{\partial\psi_2}{\partial z_2}\dot{z}_2 + \frac{\partial\psi_2}{\partial\eta_2}\dot{\eta}_2\right) - \kappa_4 z_3\end{aligned}$$

with $\kappa_4 > 0$, gives

$$\begin{aligned}\dot{V}_3 &\leq -(1-\theta_2)k_2 c_1 \eta_2^2 - \frac{1}{t_r}(1+k_4)z_3^2 \qquad (48)\\ &\quad - \left(-K_{\dot{\phi}} + k_3 - \frac{\gamma_3^2}{4\theta_2 k_2 c_1}\right)z_2^2\end{aligned}$$

which is negative definite. Hence the origin of (44) is asymptotically stable [14, Lemma 14.2] with a region of attraction that is a function of $\tau_{\max}$. Note that in (47) $\dot{z}_2$ is computed based upon the knowledge of only the states of the roll subsystem. In fact $\dot{z}_2 = \dot{\nu}_2 + \kappa_2\nu_2$, where $\dot{\nu}_2$ is given by (29b).

IV. SIMULATIONS

The designed control laws were tested carrying out simulations with the plant model. Some simulations parameters are listed in Table I, where $\dot{\alpha}_{\max}$ is the slew rate saturation, and α_{pb} is the hydraulic proportional band. The parameters referring to the container vessel can be found in [6].

The efficacy of the combined control action was evaluated comparing the responses of the plant model when only either the fin stabiliser or the speed controller were active (Figs. 2-3). The control action is activated when the roll angle ϕ is about 5°. Fig. 2 clearly shows that the control torque supplied by the fins is not enough to damp out the motion, but only a small reduction in roll oscillations can be achieved. Conversely, a small variation in ship forward

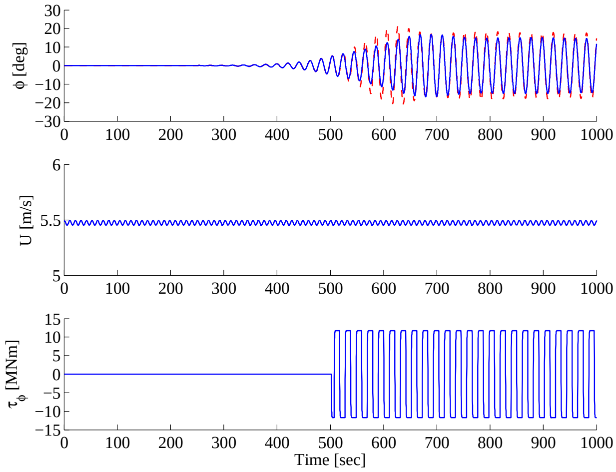

Fig. 2. Stabilisation of roll angle ϕ with only fin stabiliser active. Roll in parametric resonance (red dashed curve)

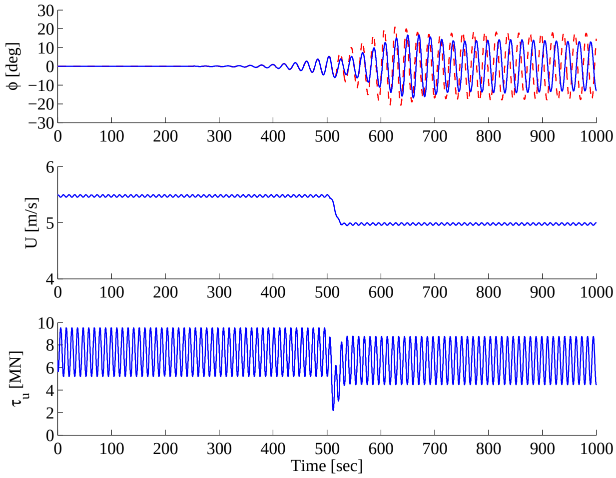

Fig. 3. Stabilisation of roll angle ϕ with only speed controller active. Roll in parametric resonance (red dashed curve)

($\Delta U = 0.5$ m/s) speed has a stronger influence in the development of parametric roll, as Fig. 3 illustrates, but it is not sufficient to bring the roll motion to zero.

Figs. 4-5 are examples of how the combined control action works. First the speed controller is activated when the roll angle is about 5°, and the ship forward speed is increased or decreased according to the new set-point. When the new forward speed set-point is about to be reached the fin stabiliser takes over driving the roll motion to zero. The efficacy and the velocity of the control action is strictly dependent on the new value of the ship forward speed. In fact, by comparing Fig. 4 with Fig. 5 it can be noticed that even if $|\Delta U| = 2$ m/s in both cases, increasing or decreasing the speed determine a different performance of the fin stabiliser, as shown by the control torque τ_ϕ supplied by the fins.

The control torque τ_ϕ depends on the amount of lift that the fins are able to produce, and this in turn is proportional to the square of the flow velocity. Therefore, increasing the ship

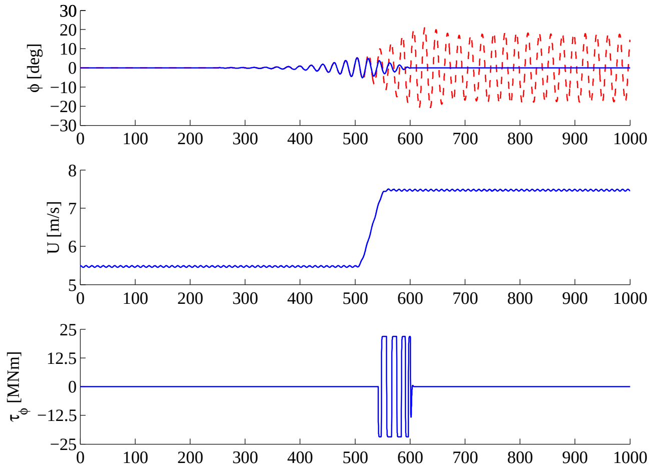

Fig. 4. Stabilisation of roll angle ϕ using the plant model ($\Delta U = 2$ m/s, $\tau_{\phi,\max} = 21.8$ MNm). Roll in parametric resonance (red dashed curve)

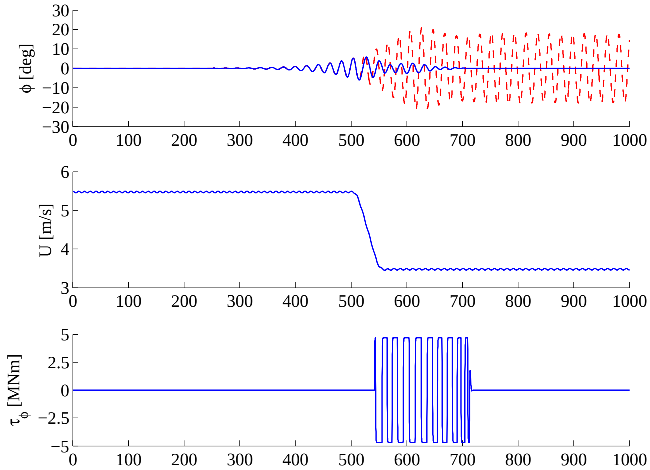

Fig. 5. Stabilisation of roll angle ϕ using the plant model ($\Delta U = -2$ m/s, $\tau_{\phi,\max} = 4.7$ MNm). Roll in parametric resonance (red dashed curve)

forward speed makes the overall control law more effective; in addition to de-tuning the frequency coupling condition $\omega_e \approx 2\omega_\phi$, it increases the maximum control torque that the fin stabiliser can supply to damp out the roll motion.

V. CONCLUSIONS

A combined speed and fin stabiliser controller was developed applying nonlinear control methods.

A nonlinear backstepping-based fin stabiliser was developed, capable of driving the roll motion asymptotically to zero in a region of attraction that is a function of the maximum control moment the fins can supply.

A speed controller was developed applying classical Lyapunov stability theory. In the presence of a permanent time-varying disturbance (i.e. waves) this controller guarantees that the surge speed is globally uniformly ultimately bounded, where the ultimate bound is a function of the disturbance amplitude.

The combined action of the two controllers stabilised the roll motion in parametric resonance condition. Moreover, the performance of the fin stabiliser was improved by the speed controller, because positive variations in forward speed allowed for a larger control torque.

These results were verified by simulating the combined control law with a high fidelity model.

APPENDIX

A. Time-varying disturbance

The disturbance acting on the surge subsystem is given by

$$
\begin{aligned}
e_1(\nu_1, t) &= F_x^{FK} \\
&= \gamma_1(\omega + k\nu_1)[\sin(\omega t + kL_s + k\eta_1) \\
&\quad - \sin(\omega t + k\eta_1)] \\
&= \gamma_1\omega[\sin(\omega t + kL_s + k\eta_1) - \sin(\omega t + k\eta_1)] \\
&\quad + \gamma_1 k z_1[\sin(\omega t + kL_s + k\eta_1) - \sin(\omega t + k\eta_1)] \\
&\quad + \gamma_1 k \nu_d[\sin(\omega t + kL_s + k\eta_1) - \sin(\omega t + k\eta_1)].
\end{aligned}
\tag{49}
$$

Since the following trigonometry relationship holds

$$\sin\alpha - \sin\beta \le |\sin\alpha - \sin\beta| \le |\sin\alpha| + |-\sin\beta| \le 2,$$

then the time-varying disturbance satisfies the following inequality

$$
\begin{aligned}
e_1(\nu_1, t) &\le 2\gamma_1\omega + 2\gamma_1 k z_1 + 2\gamma_1 k \nu_d \\
&\le 2\gamma_1\omega + 2\gamma_1 k z_1 + 2\gamma_1 k \nu_{d,\max}
\end{aligned}
\tag{50}
$$

where $\nu_{d,\max}$ is the upper bound of the reference trajectory.

REFERENCES

[1] A. Tondl, T. Ruijgrok, F. Verhulst, and R. Nabergoj, *Autoparametric Resonance in Mechanical Systems*. Cambridge University Press, 2000.

[2] R. Grimshaw, *Nonlinear Ordinary Differential Equations*. CRC Press, 1993.

[3] W. N. France, M. Levadou, T. W. Treakle, J. R. Paulling, R. K. Michel, and C. Moore, "An investigation of head-sea parametric rolling and its influence on container lashing systems," in *SNAME Annual Meeting*, 2001.

[4] S. M. Carmel, "Study of parametric rolling event on a panamax container vessel," *Journal of the Transportation Research Board*, vol. 1963, pp. 56–63, 2006.

[5] C. Holden, R. Galeazzi, T. I. Fossen, and T. Perez, "Stabilization of parametric roll resonance with active u-tanks via lyapunov control design," in *Proc. of the 10th European Control Conference*, 2009.

[6] C. Holden, R. Galeazzi, C. Rodríguez, T. Perez, T. I. Fossen, M. Blanke, and M. A. S. Neves, "Nonlinaer container ship model for the study of parametric roll resonance," *Modeling, Identification and Control*, vol. 28, pp. 87–113, 2007.

[7] R. Galeazzi, J. Vidic-Perunovic, M. Blanke, and J. J. Jensen, "Stability analysis of the parametric roll resonance under non-constant ship speed," in *Proc. of the 9th Biennial ASME Conference on Engineering Systems Design and Analysis*, 2008.

[8] M. Blanke, K. P. Lindegaard, and T. I. Fossen, "Dynamic model for thrust generation of marine propellers," in *Proc. of the IFAC Conference on Manoeuvreing and Control of Marine Craft*, 2000.

[9] J. N. Newman, *Marine Hydrodynamics*. The MIT Press, 1977.

[10] J. J. Jensen, P. T. Pedersen, and J. Vidic-Perunovic, "Estimation of parametric roll in stochastic seaway," in *Proc. of IUTAM Symposium on Fluid-Structure Interaction in Ocean Engineering*, 2008.

[11] R. Galeazzi and M. Blanke, "On the feasibility of stabilizing parametric roll with active bifurcation control," in *Proc. of the 7th IFAC Conference on Control Applications in Marine Systems*, 2007.

[12] T. Perez, *Ship Motion Control*. Springer, 2005.

[13] J. van Amerongen, P. G. M. van der Klugt, and H. R. van Nauta Lemke, "Rudder roll stabilization for ships," *Automatica*, vol. 26(4), pp. 679–690, 1990.

[14] H. K. Khalil, *Nonlinear Systems 3^{rd} edition*. Prentice Hall, 2002.